AD-A050 297 OREGON GRADUATE CENTER . BEAVERTON F/G 7/2
MECHANISM OF SINGLET OXYGEN GENERATION BY CHEMICAL REACTIONS. (U)
OCT 77 J K HURST AFOSR-75-2821
UNCLASSIFIED AFOSR-TR-78-0113 NL

| OF |
AD A050297

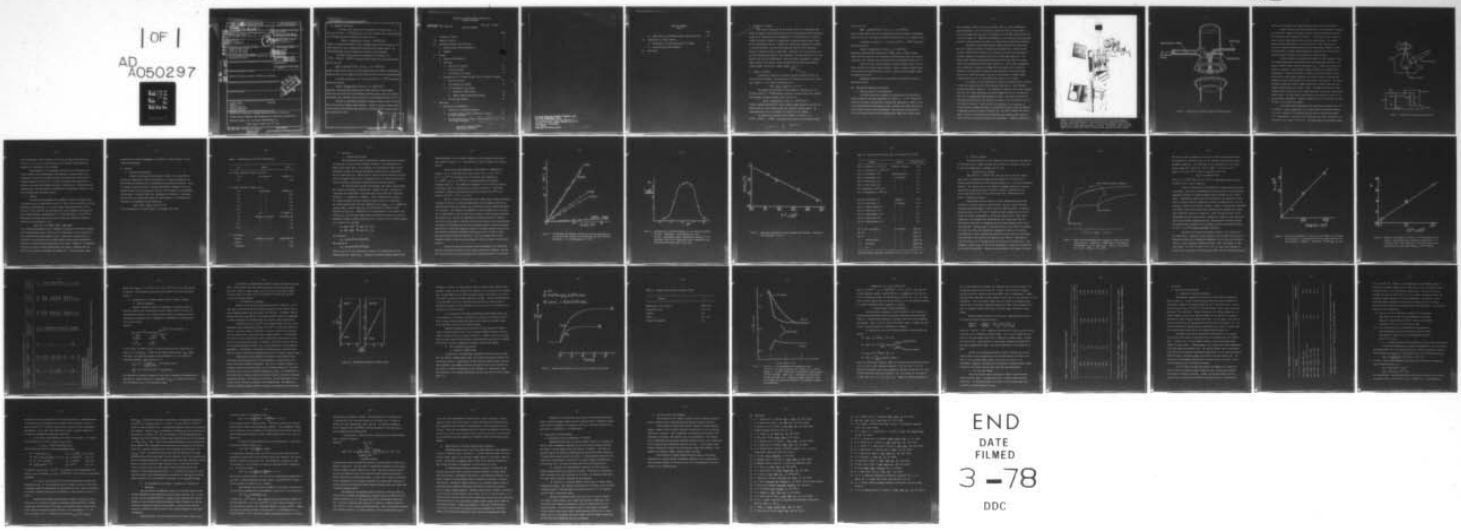

END
DATE FILMED
3-78
DDC

UNCLASSIFIED

SECURITY CLASSIFICATION OF THIS PAGE (When Data Entered)

REPORT DOCUMENTATION PAGE

READ INSTRUCTIONS BEFORE COMPLETING FORM

1. REPORT NUMBER: AFOSR-TR-78-0113
2. GOVT ACCESSION NO.
3. RECIPIENT'S CATALOG NUMBER
4. TITLE (and Subtitle): MECHANISM OF SINGLET OXYGEN GENERATION BY CHEMICAL REACTIONS
5. TYPE OF REPORT & PERIOD COVERED: Final rept. 6 Jun 75 - 31 May 77
6. PERFORMING ORG. REPORT NUMBER
7. AUTHOR(s): James K. Hurst
8. CONTRACT OR GRANT NUMBER(s): AFOSR-75-2821
9. PERFORMING ORGANIZATION NAME AND ADDRESS: Oregon Graduate Center, 19600 N.W. Walker Rd., Beaverton, OR 97005
10. PROGRAM ELEMENT, PROJECT, TASK AREA & WORK UNIT NUMBERS: 61102F; 2303/B1
11. CONTROLLING OFFICE NAME AND ADDRESS: Air Force Office of Scientific Research/NC, Bolling AFB DC 20332
12. REPORT DATE: 31 Oct 77
13. NUMBER OF PAGES: 48
14. MONITORING AGENCY NAME & ADDRESS (if different from Controlling Office)
15. SECURITY CLASS. (of this report): UNCLASSIFIED
15a. DECLASSIFICATION/DOWNGRADING SCHEDULE

16. DISTRIBUTION STATEMENT (of this Report)

Approved for public release; distribution unlimited.

17. DISTRIBUTION STATEMENT (of the abstract entered in Block 20, if different from Report)

18. SUPPLEMENTARY NOTES

19. KEY WORDS (Continue on reverse side if necessary and identify by block number)

Singlet Oxygen
Kinetics
Chemical Reaction
Oxidation-Reduction
Hydrogen Peroxide
Chlorine

20. ABSTRACT (Continue on reverse side if necessary and identify by block number)

Hypochlorite oxidation of hydrogen peroxide proceeds by three concurrent reaction pathways, each giving rise to quantitative production of molecular oxygen, i.e., an overall stoichiometery of:

$$HOCl + H_2O_2 \longrightarrow H_2O + O_2 + H^+ + Cl^-$$

DD FORM 1 JAN 73 1473 EDITION OF 1 NOV 65 IS OBSOLETE

UNCLASSIFIED

SECURITY CLASSIFICATION OF THIS PAGE (When Data Entered)

390044

AD A050297

AU NU.

DDC FILE COPY

DDC DRAPER FEB 23 1978 F

20. ABSTRACT (Continued)

In strongly acid solutions in the presence of chloride ion, i.e., for which $(H^+)(Cl^-) > 10^{-5}M^2$, molecular chlorine is formed which reacts rapidly with hydrogen peroxide according to the rate law (5):

$$dO_2/dt = k_1(H_2O_2)(Cl_2), \text{ with } k_1 = 1.9\times10^2M^{-1}sec^{-1}$$

Chemical trapping experiments to detect singlet oxygen formation could not be made because Cl_2 reacts competitively with available trapping agents. No chemiluminescence could be observed for reaction by this pathway.

In weakly acid solutions in the presence of chloride, i.e., $10^{-5}M^2 > (H^+)(Cl^-) > 10^{-8}M^2$, a relatively slow reaction can be detected which has the rate law

$$dO_2/dt = k_2(HOCl)(H^+)(Cl^-), \text{ with } k_2 = 3.5 \times 10^4M^{-2}sec^{-1}$$

Singlet oxygen yields could not be determined because the chemical intermediate defined by the rate law (H_2OCl_2) reacted preferentially with the trapping agents

In alkaline solutions, i.e., for which $(H^+)(Cl^-) < 10^{-8}M^2$ the pathway having the rate law:

$$dO_2/dt = k_3(H_2O_2)(OCl^-), \text{ with } k_3 = 3.3 \times 10^3M^{-1}sec^{-1}$$

dominates, producing nearly quantitative (>90%) yields of singlet oxygen. (Rate laws are written for the predominant reaction species under the reaction conditions; rate constants refer to reaction in 0.1M phosphate buffer at 25°.)

Reaction by the alkaline pathway in aqueous alcoholic media also gave nearly quantitative singlet oxygen formation. Redox in nonpolar aprotic media, solvents which would minimize deactivation of initially formed singlet oxygen, was prohibitively slow.

MECHANISM OF SINGLET OXYGEN GENERATION BY CHEMICAL REACTIONS

AFOSR-TR- 78-0113

AFOSR 75-2821

TABLE OF CONTENTS

AIR FORCE OFFICE OF SCIENTIFIC RESEARCH (AFSC)
NOTICE OF TRANSMITTAL TO DDC
This technical report has been reviewed and is
approved for public release IAW AFR 190-12 (7b).
Distribution is unlimited.
A. D. BLOSE
Technical Information Officer

TABLE OF CONTENTS
Page 2

I. Statement of Purpose

The overall objectives of the present work are to investigate mechanisms of chemical reactions which give rise to electronically excited molecular oxygen and to determine factors responsible for its deactivation in solution, thereby providing the means for optimization of gaseous singlet oxygen formation by homogeneous reaction. Studies have focused upon hypochlorite oxidation of hydrogen peroxide, this reaction having been shown to yield substantial amounts of singlet molecular oxygen (1-3). Inasmuch as the redox kinetics were not well-characterized (3-5), we have undertaken a thorough analysis of the rate behavior and reaction stoichiometry. Where tractable, measurement of singlet oxygen yields by the various reaction pathways has been made using chemical trapping agents selective for singlet oxygen.

II. Summary of Results

Hypochlorite oxidation of hydrogen peroxide proceeds by three concurrent reaction pathways, each giving rise to quantitative production of molecular oxygen, i.e., an overall stoichiometry of:

$$HOCl + H_2O_2 \longrightarrow H_2O + O_2 + H^+ + Cl^-$$

In strongly acid solutions in the presence of chloride ion, i.e., for which $(H^+)(Cl^-) > 10^{-5}M^2$, molecular chlorine is formed which reacts rapidly with hydrogen peroxide according to the rate law (5):

$$dO_2/dt = k_1(H_2O_2)(Cl_2), \text{ with } k_1 = 1.9\times10^2 M^{-1}sec^{-1}$$

Chemical trapping experiments to detect singlet oxygen formation could not be made because Cl_2 reacts competitively with available trapping agents. No chemiluminescence could be observed for reaction by this pathway.

In weakly acid solutions in the presence of chloride, i.e., $10^{-5}M^2 > (H^+)(Cl^-) > 10^{-8}M^2$, a relatively slow reaction can be detected which

has the rate law

$$dO_2/dt = k_2(HOCl)(H^+)(Cl^-), \text{ with } k_2 = 3.5 \times 10^4 M^{-2} sec^{-1}$$

Singlet oxygen yields could not be determined because the chemical intermediate defined by the rate law (H_2OCl_2) reacted preferentially with the trapping agents.

In alkaline solutions, i.e., for which $(H^+)(Cl^-) < 10^{-8} M^2$ the pathway having the rate law:

$$dO_2/dt = k_3(H_2O_2)(OCl^-), \text{ with } k_3 = 3.3 \times 10^3 M^{-1} sec^{-1}$$

dominates, producing nearly quantitative (>90%) yields of singlet oxygen. (Rate laws are written for the predominant reaction species under the reaction conditions; rate constants refer to reaction in 0.1M phosphate buffer at 25°.)

Reaction by the alkaline pathway in aqueous alcoholic media also gave nearly quantitative singlet oxygen formation. Redox in nonpolar aprotic media, solvents which would minimize deactivation of initially formed singlet oxygen, was prohibitively slow.

Mechanistic implications of the results are discussed in detail in following sections.

III. Experimental Methods and Procedures

A. Reaction Rates and Stoichiometries

A variable-speed drive assembly for mixing reactants under widely-varying conditions has been constructed (6) (Figure 1). In the configuration shown the instrument has been used in quench-flow experiments to measure rates of peroxide-hypochlorite decomposition and to provide controlled, uniform mixing in singlet oxygen trapping experiments. The reactions of hypochlorous acid with hydrogen peroxide and 2,5-dimethylfuran (DMFu) were studied using

this instrument coupled to 0.1-1.0 cm optical cells in a Cary 16 absorption spectrophotometer. Loss of ClO^- ions was followed at 290 nm, loss of DMFu at 215 nm, and appearance and decay of intermediates in the DMFu oxidation reaction at 240 nm (Figure 12). Additional measurements of the relatively rapid H_2O_2-HOCl reaction in alkaline media were made on a Gibson-Durrum stopped-flow instrument.

Experiments in gas phase singlet oxygen production were made using the drive assembly attached to a mixing cell equipped with a nozzle directed to spray rapidly mixed solutions into a liquid N_2 cold trap with simultaneous cryogenic pumping of uncondensed gases into a vacuum pump (Figure 2). Gas-phase singlet oxygen was detected downstream from the cold trap by the observation of violanthrone-catalyzed dimol emission (7). Filter paper impregnated with violanthrone, (prepared by soaking the filter paper with a chloroform solution of recrystallized violanthrone and evaporating off the chloroform) placed in the exit-tube showed a red glow in the presence of singlet oxygen concentrations too low for spontaneous dimol emission to be visible.

An assembly for the measurement of oxygen concentrations which utilizes a Clark-type oxygen electrode (Yellow Springs Instrument Co., Model YS-4004) has been constructed (Figure 3). The electrode is inserted into a pyrex jacketed cell (22.5 ml volume) maintained at constant temperature by the circulation of water from a thermostatted bath through the jacket. The oxygen electrode response was monitored with a 1 mv recorder interfaced to the electrode by the circuit shown in Figure 3. The instrument was calibrated by the injection of a known volume of oxygen-saturated or air-saturated solvent, and by the addition of hydrogen peroxide followed by catalase (8). The system response was tested under a variety of conditions and no deviations from linearity were found for the pH and salt concentrations used in the experiments. Changes in sensitivity

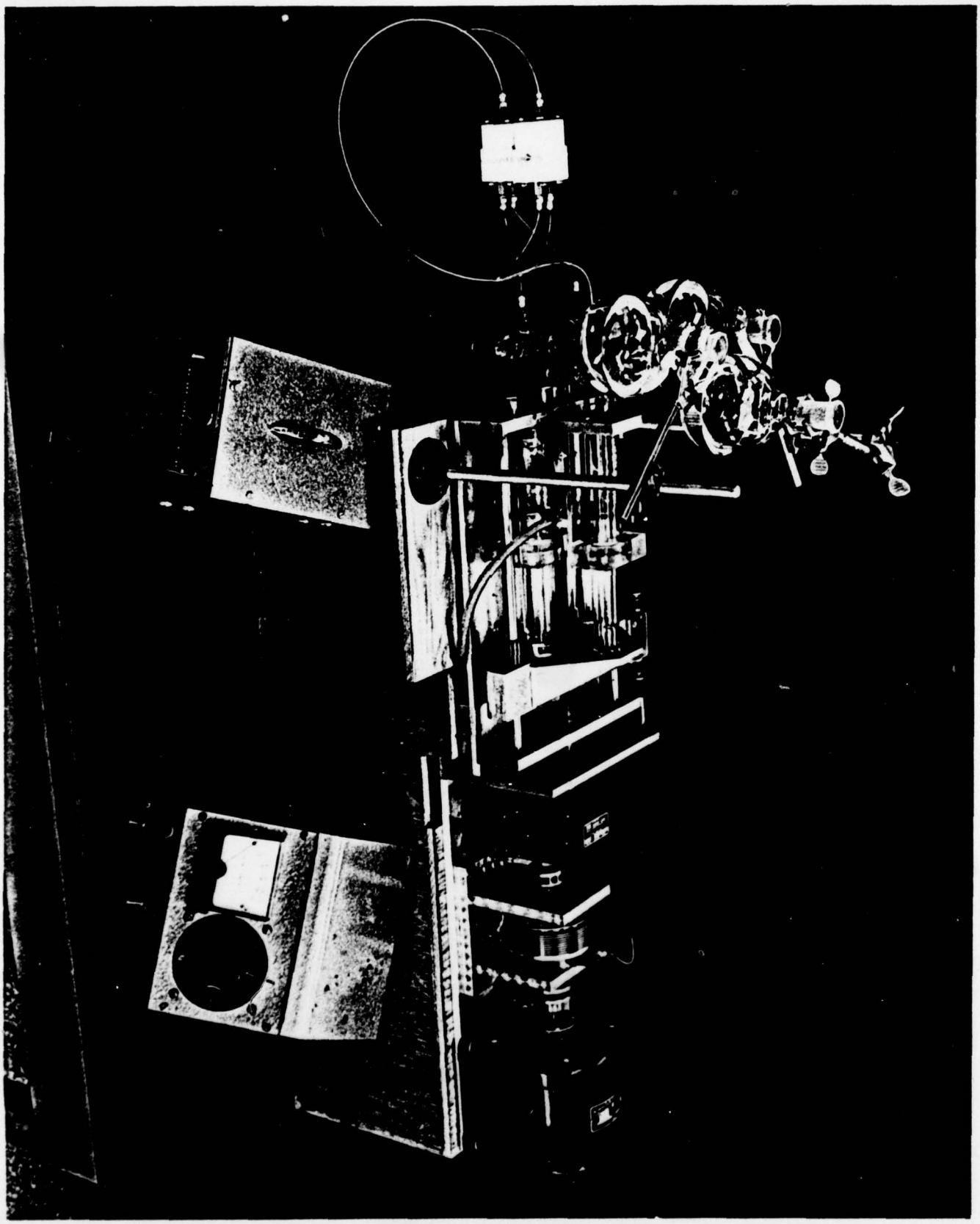

Figure 1. Drive Assembly Equipped for Quench-Flow Kinetic Measurements. Left to right: motor, magnetic slip-clutch, gear box, pushplate with drive syringes (3), reagent resevoir flasks, tandem mixing chambers, quartz optical cuvette for in situ spectrophotometric analyses. Foreground: motor variable-speed control (left) and clutch variable-torque control circuitry (right).

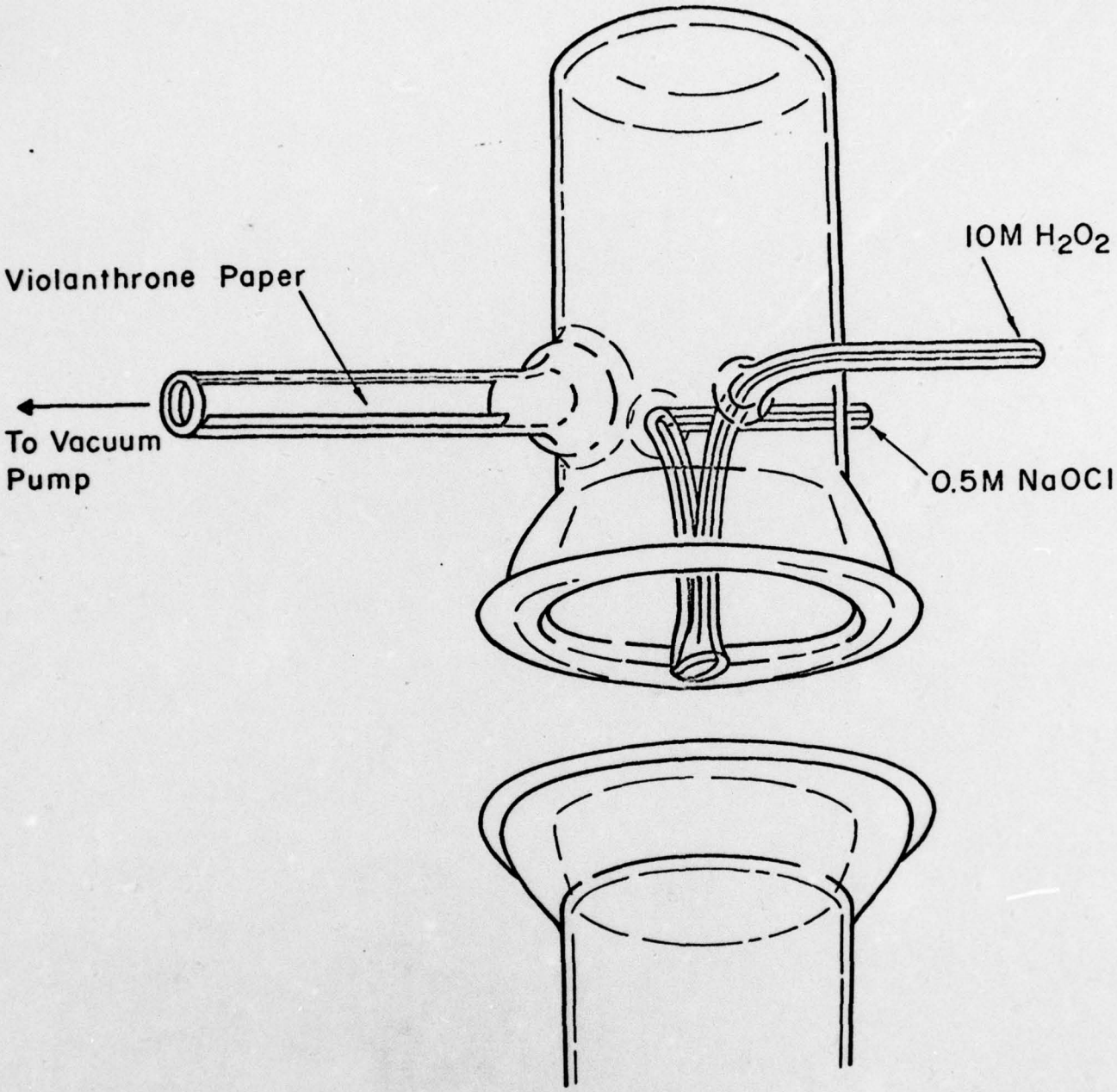

Figure 2. Mixing Cell for Gaseous Singlet Oxygen Generation

with solvent composition and temperature were dealt with by recalibration.

Oxygen formation rates and stoichiometries were determined by injection of hypochlorite reagent into hydrogen peroxide solutions which had previously been deoxygenated by bubbling with nitrogen. Concentrations were adjusted to ensure that electrode response times were not rate-limiting. For singlet oxygen trapping experiments, the rate of solution of DMFu required that at least ten minutes preequilibration time be taken between addition of DMFu and hypochlorite. Singlet oxygen trapped was calculated from the difference between hypochloride added and (ground-state) oxygen measured.

Earlier attempts at determining the extent of DMFu trapping of singlet oxygen employed gas chromatographic and spectrophotometric methods. The acceptor molecule gives strong uv absorption (ε_{215} = 7,900) and is easily resolved on carbowax or porous polymer columns, allowing for straightforward determination of DMFu concentrations. However, no reaction product could be identified by either method, requiring that product yields be inferred from changes in acceptor concentration over the course of the reaction. For the experimental conditions required, DMFu concentrations undergo relatively small changes during reaction with singlet oxygen. Subsequent manipulative losses stemming from the high volatility of DMFu give rise to relatively large experimental errors. For this reason, these methods were abandoned in favor of the in situ oxygen measurements. Results obtained by the various methods are qualitatively in accord with one another.

Photosensitization experiments were conducted by measuring the rate of change of oxygen concentration of a solution within the constant-temperature-cell containing 10^{-6}M methylene blue and various known concentrations of 2,5-dimethylfuran. The source of illumination was a 200 w lamp placed approximately four inches from the cell. By adding methyl red and methyl orange

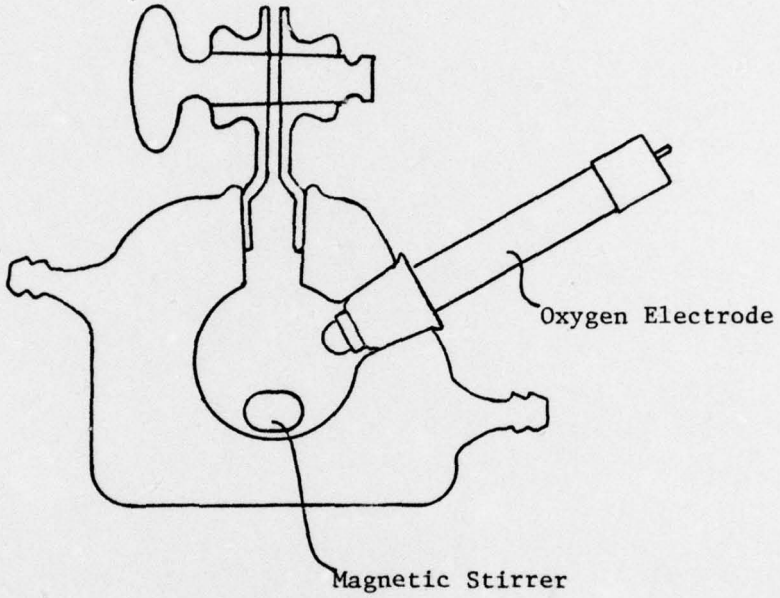

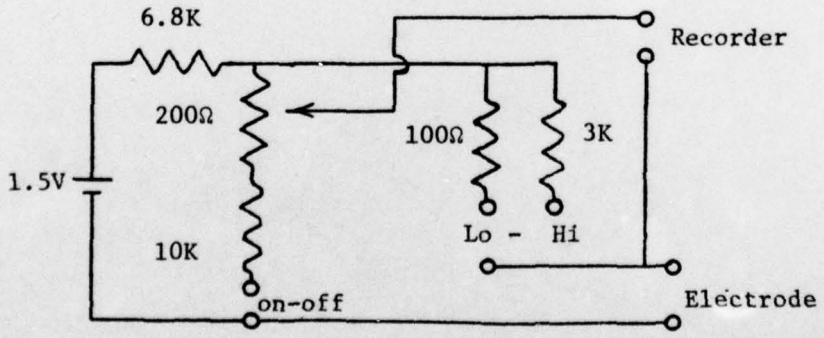

Figure 3. Oxygen Cell and Associated Circuitry

to the surrounding coolant solution, all but the red light was filtered out. Photolysis of the methylene blue solution in the absence of quenching agent resulted in no significant loss of oxygen.

Stoichiometries for the H_2O_2-HOCl reaction over a wide range of reaction conditions were established by determination of oxygen yields, by determination of chloride ion formation using an ion-selective electrode and by standard iodometric titration (9). For the last method, known quantities of reactants were mixed with hydrogen peroxide in slight excess. Hydrogen peroxide remaining after reaction ceased was determined by I_2-thiosulfate titration. The various methods gave equivalent results.

B. Reagents

Previous work had suggested that commercial sources of reagents were of suitable purity for quantitative study (3). Raman infra-red analysis of sodium hypochlorite (Mallinckrodt, A. R.) gave spectral lines characteristic of OCl^- (713 cm^{-1}), ClO_2^- (790 cm^{-1}) and ClO_3^- (930 cm^{-1}) ions; iodometric titrations (9) gave estimated relative concentrations of $Cl^-:ClO^-:ClO_2^-:ClO_3^- = 1:0.45:10^{-3}:0.2$. Hypochlorite solutions used in the present studies were therefore prepared by reaction of Cl_2 with HgO (8); i.e.,

$$H_2O + 2Cl_2 + (n+1)HgO \rightarrow 2HOCl + HgCl_2 \cdot nHgO$$

or by vacuum distillation at 40° of commercial 5% hypochlorite solution acidified to pH 6 with phosphoric acid. The 0.3 to 0.5 M hypochlorite stock solutions were kept refrigerated and were replaced monthly. Experiments requiring very low chloride ion concentrations were run with either freshly prepared hypochlorite solutions or those previously treated with silver oxide. Commercial 2,5-dimethylfuran was purified by column chromatography over alumina. Methylene blue was purified by the method of Bergmann and O'Konski (11). Water was either twice

distilled over alkaline permanganate or purified by reverse osmosis - ion exchange chromatography.

IV. Results

A. Reaction Stoichiometries

Results of the various stoichiometric analyses of the H_2O_2-HOCl reactions are summarized in Table I; the data refer to reaction conditions for which either the alkaline (k_3) or intermediate (k_2) pathways predominate. Thus, in contrast to previous reports of excess hypochlorite consumption for the k_2 pathway (5) and for the k_3 pathway in D_2O (3), we find simple 1:1 stoichiometry is maintained. Previous studies (12), subsequently confirmed (5), have shown that the acid (k_1) pathway also obeys this stoichiometry; it is therefore evident that by all pathways the net reaction is:

$$H_2O_2 + HOCl \longrightarrow O_2 + H_2O + H^+ + Cl^-$$

or its equivalent for the other forms of the oxidant (Cl_2, OCl^-).

Table I. Stoichiometry of the H_2O_2- HOCl Reaction

pH	Method	Ratio
a) In H_2O, 0.1M PO_4^{3-} buffer, 0.1 M Cl^-:		
3.75	O_2-electrode	O_2:HOCl=1.0_4
4.0	" "	1.0_6
b) In H_2O, 0.1M PO_4^{3-} buffer, no Cl^-:		
3.9	O_2-electrode	O_2:HOCl=1.0_o
5.0	" "	0.9_8
6.0	" "	0.9_7
7.0	" "	0.9_7
7.8	" "	1.0_o
10.3	" "	1.0_2
7-9	Cl^- "	Cl^-:HOCl=1.0_o
7.4	Iodometric titration	H_2O_2:HOCl=1.0_3
9.2	" "	1.0_5
10.5	" "	1.0_1
11.7_3	" "	1.0_8
c) In alcohols:		
Methanol	Iodometric titration	H_2O_2:HOCl=0.98
Ethanol	" "	0.97
Isopropanol	" "	0.96

B. Rate Laws

1. Alkaline (k_3) Pathway:

Spectrophotometric and O_2-potentiometric methods were used to monitor the reaction, the latter method allowing extension of the measurements into weakly acidic media (pH>3, at low chloride ion concentrations) where spectrophotometric methods fail because equilibrium concentrations of hypochlorite ion are undetectably low. Earlier work in alkaline solution had given conflicting and incomplete results (3-5); as detailed below, our present analysis indicates the pathway is described by simple mixed secord-order kinetics.

All solutions were buffered with phosphate ion; buffer concentrations were adjusted to maintain a constant ionic strength (μ=0.1M). Peroxide concentrations were maintained in sufficient excess that first-order conditions obtained; i.e., $-d(HOCl)/dt = k'(HOCl)_o$. Plots of measured rate constants (k') against hydrogen peroxide concentration were linear with intercepts at the origin demonstrating first-order dependence upon $(H_2O_2)_o$., i.e., $-d(HOCl)/dt= k_o(H_2O_2)_o(HOCl)_o$, where $k'=k_o(H_2O_2)_o$ and the subscripts o refer to total reactant concentrations. Examination of the pH dependence of the specific rate constant, k_o, over the range $3 \leq pH \leq 13$ gave rate behavior indicative of reaction principally through a pathway involving loss of a proton in the activated complex, e.g., either of the reactions

a) $H_2O_2 + OCl^- \xrightarrow{k_a} H_2O + Cl^- + O_2$

b) $HO_2^- + HOCl \xrightarrow{k_b} H_2O + Cl^- + O_2$

For reaction a,

$$k_o = k_a/(1+(H^+)/K_1)(1+K_2/(H^+)).$$

For reaction b,

$$k_o = k_b/(1+K_1/(H^+))(1+(H^+)/K_2);$$

where K_1, K_2 are the acid dissociation constants for hypochlorous acid and hydrogen peroxide, respectively. Although the reaction schemes are kinetically

indistinguishable, we will present arguments in the Discussion Section which favor reaction scheme b; i.e., identification of HO_2^- and HOCl as the reactive species.

Data from the spectrophotometric measurements are summarized in Figures 4 and 5. Using literature values (13,14) for $K_1 = 2.9 \times 10^{-8}$ M, $K_2 = 2.2 \times 10^{-12}$ M, we calculate for the specific rate constants $k_a = 3.4 \times 10^3 M^{-1}$, $k_b = 4.4 \times 10^7 M^{-1}sec^{-1}$, in good agreement with previous estimated values (3). The temperature dependence for this reaction, measured by following rates of oxygen evolution, is given in Figure 6. Activation parameters, calculated from absolute reaction rate theory, are $\Delta H^{\circ\neq} = 10.1$ kcal/mole and $\Delta S^{\circ\neq} = -19.1$ e.u. at 25°.

Results of kinetic studies made over a wider range of medium conditions, including the low pH, low chloride measurements with the oxygen electrode, are reported in Table II; rate constants (k_b) have been calculated assuming mechanism b is operative. The reaction is insensitive to ionic strength and to the identity of added buffers, with the exception of borate ion whose presence decreases the reaction rate. Borate ion complexation of hydrogen peroxide is known to occur (15); the decrease in reaction rate in borate buffers can be quantitatively accounted for by assuming that the borate-peroxide complex is unreactive towards hypochlorite, thereby decreasing the "effective" hydrogen peroxide concentration. The dissociation constant calculated from the rate data is 0.037M, in agreement with literature value of 0.03M (15). It is also notable that acetate catalysis observed for the acid (k_1) pathway (5) does not extend to the alkaline reaction.

Because the reaction rate shows strong pH dependence, rate variations observed for different solvents are not easily interpreted; in general, the reaction rate was found to decrease markedly with decreasing polarity of the solvent.

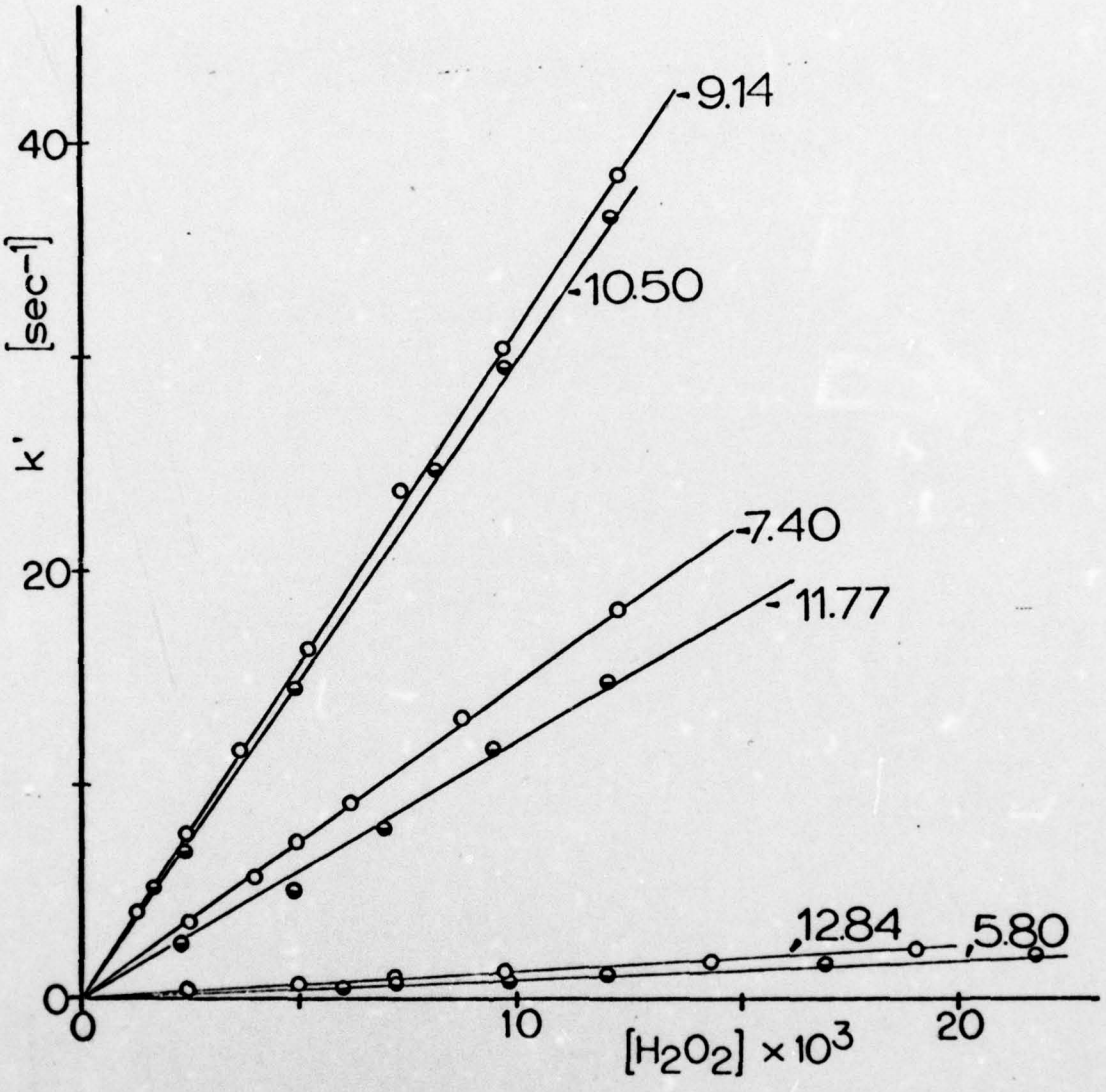

Figure 4. pH Dependence and Hydrogen Peroxide Concentration Dependence of the Observed Rate Constant for the Alkaline H_2O_2-HOCl Reaction. Conditions: μ = 0.1M (phosphate), T = 25°C.

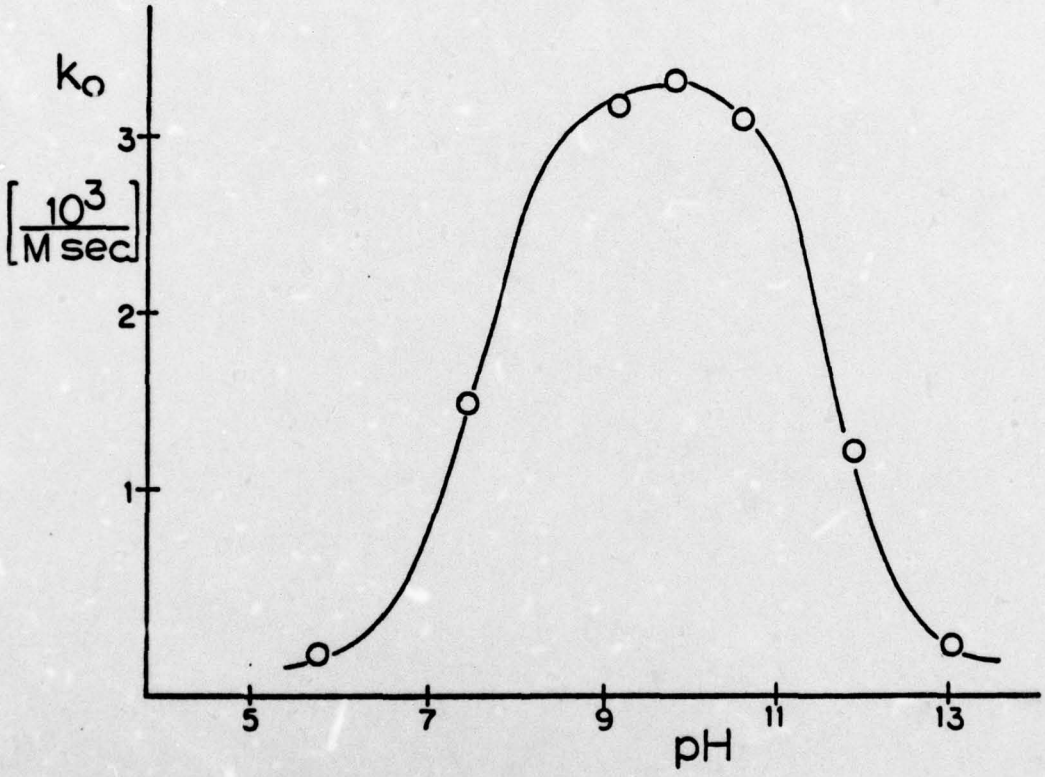

Figure 5: pH-Dependence of the Rate Constant for the Alkaline H_2O_2-HOCl Reaction. Conditions: μ=0.1M (phosphate), T=25°. Circles - experimental points, representing averages of 6-10 individual runs; line - theoretical curve, assuming rate and equilibrium parameters given in the text.

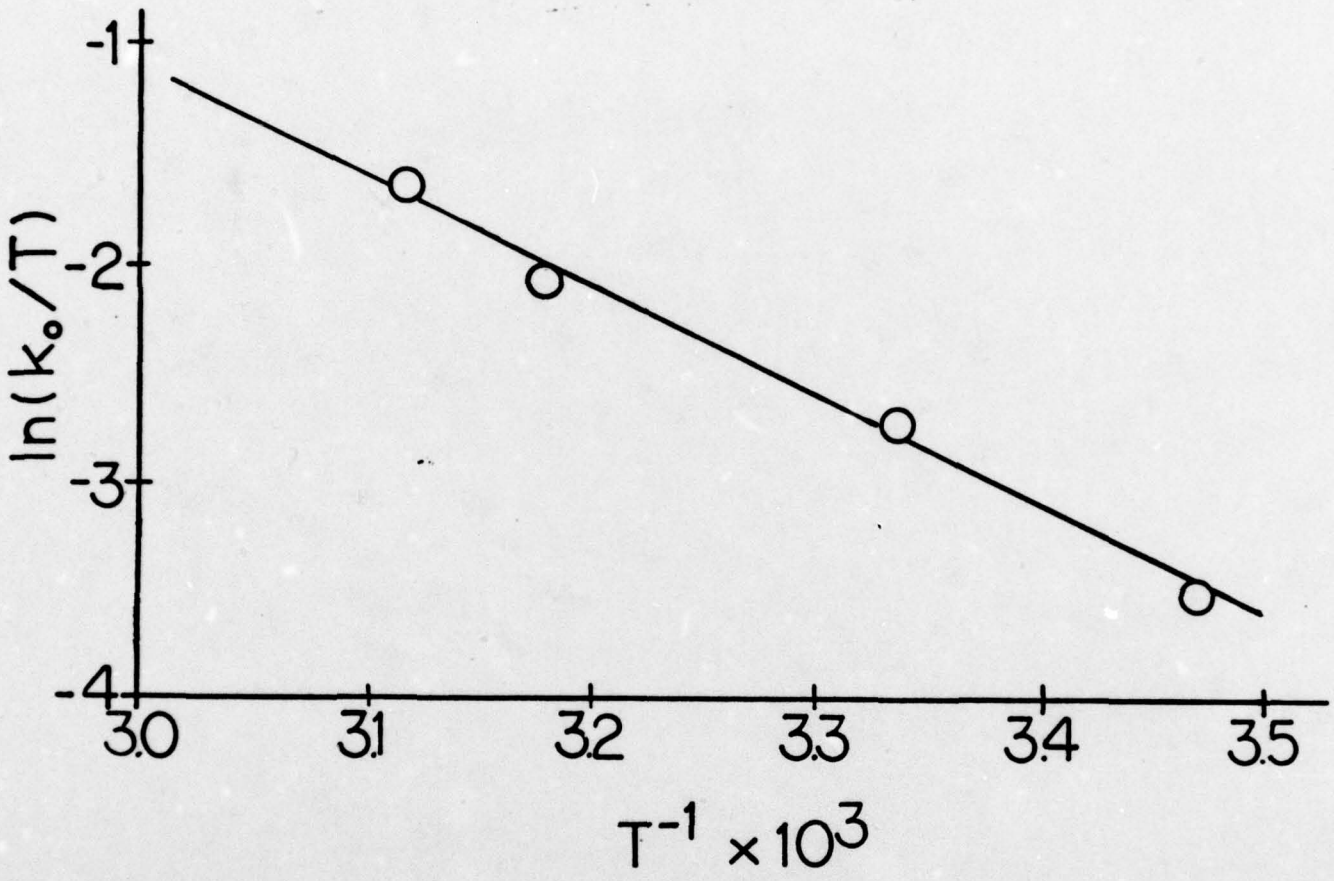

Figure 6. Temperature Dependence of the k_3 Pathway Rate Constant. Conditions: 0.1M (phosphate), pH 5.0.

Table II. Specific Rate Constants (k_b) for the Alkaline Reaction[a]

Medium	Method	$10^{-7} k_b$ ($M^{-1} sec^{-1}$)
pH 4-5, unbuffered, $\mu \approx 10^{-4}$ M, 25°	Iodometric titration	3.2[b]
pH 7-13, unbuffered, 1 $\mu \approx 10^{-4}$ M, 25°	" "	$\sim$ 3[c]
pH 5, 0.1M phosphate, 25°	Spectrophotometric	4.2
pH 4, 0.1M phosphate, 25°	O_2 evolution	4.2
pH 4, 0.025M acetate, 25°	" "	4.3
pH 9.4, 0.1M acetate, 25°	" "	4.2
pH 4, unbuffered, $\mu \approx 10^{-4}$ M, 25°	" "	4.6
pH 3.7, unbuffered, $\mu \approx 10^{-4}$ M, 25°	" "	4.0
pH 6-12, 0.1M borate, 0°	Manometry	(<1)[d]
pH 9.2, 0.04M borate, 8°	O_2 evolution	0.46
pH 9.2, 0.04M phosphate, 8°	" "	1.6
pH 9.2, 0.04M borate, 19°	" "	1.7
pH 9.2, 0.04M phosphate, 19°	" "	2.9
pH 9.2, 0.04M borate, 25°	" "	2.5
pH 9.2, 0.04M phosphate, 25°	" "	3.9
pH 4.5, methanol:H_2O=1:1	O_2 evolution	$t_{1/2} \cong 60$ sec
pH 8.25, " " "	" "	$t_{1/2} \cong 30$ sec
pH 9.0, " " "	" "	$t_{1/2} \cong 15$ sec
--- ethanol:H_2O=19:1	" "	$t_{1/2} \cong 10^2$ sec
--- n-propanol	" "	$t_{1/2} > 10^2$ sec
--- CCl_4	" "	$t_{1/2} > 10^3$ sec

[a]Unless otherwise indicated, this work; [b] ref. 5; [c] ref. 3, [d] ref. 16.

2. Acid (k_1) Pathway

The kinetic-behavior of this pathway has been thoroughly described (5); our measured rates of oxygen evolution were identical to previously cited rates of chlorine disappearance, confirming the rate law.

3. Intermediate (k_2) Pathway

When $(H^+)(Cl^-) = 10^{-8}$-10^{-5} M^2, the total rate of reaction, though quite slow, is significantly higher than accountable by the reactions of chlorine and hypochlorite ion with hydrogen peroxide, i.e., the acid and alkaline pathways. The reaction rate in this region is extremely sensitive to environmental effects, exhibiting buffer catalysis, apparent autoinhibition and very strong inhibition by certain cations and anions. Representative behavior is exhibited in Figure 7.

Reproducible rates not subject to these complicating effects were observed for the early stages of the reactions. The rate law was therefore determined from measurement of initial rates of oxygen evolution. At absolute rates exceeding 1.5×10^{-7} M sec^{-1}, oxygen electrode response was too slow to provide an accurate measurement of the initial reaction rates. Under these conditions, rate constants were determined from the slopes taken over the first several half-lives of integrated rate plots made assuming simple first-order behavior. This procedure is justified because we had found by the method of initial rates that the concentration dependence of HOCl was first-order, concentrations of other reactants were invariant and the reaction stoichiometry was unaffected by the catalytic and inhibitory rate effects. Excepting the first few points, the first-order plots were linear over 2-3 half-lives. Order dependence on HOCl, H_2O_2, H^+ and Cl^- was determined by varying the concentration of each species separately. Significant contributions to the overall rate were

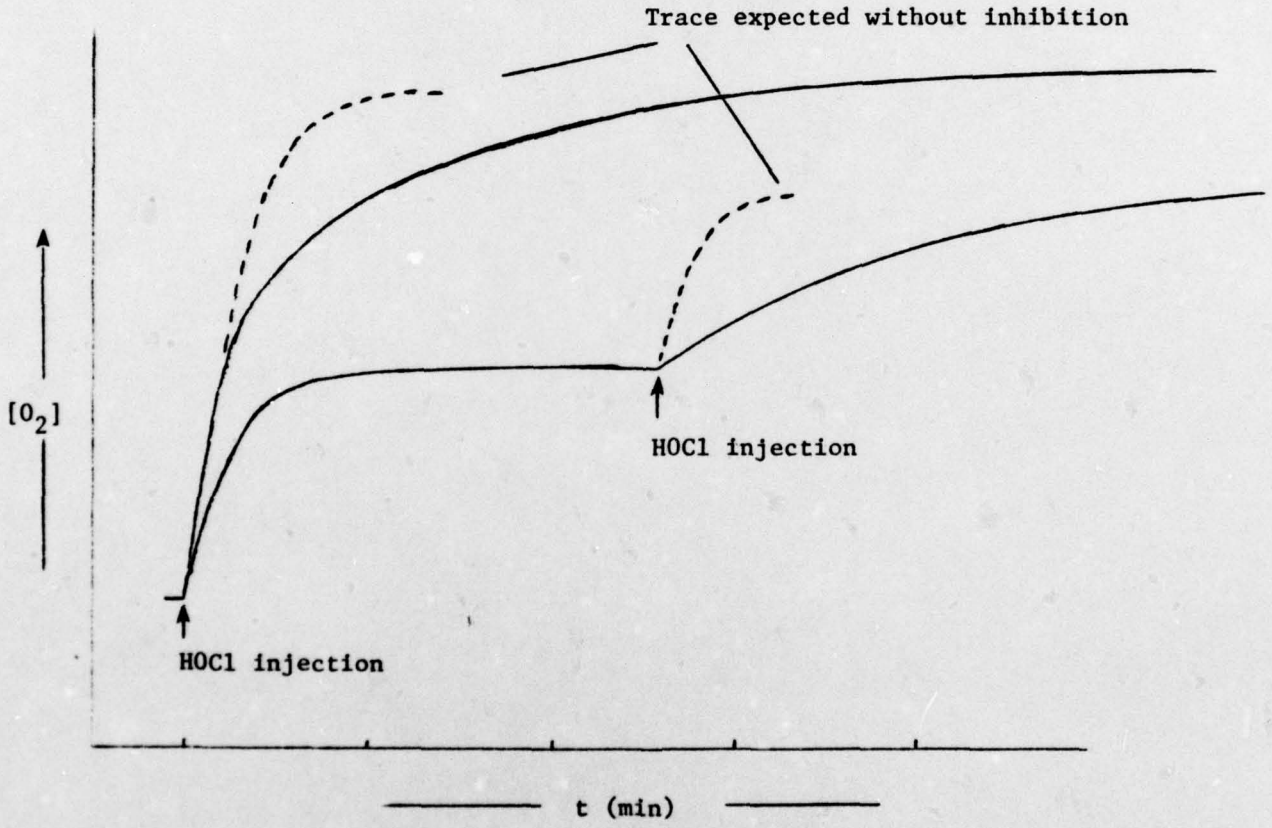

Figure 7. Oxygen Electrode Response After Injection of HOCl into 0.0013 M H_2O_2 Solution. Conditions: 0.0048M NaCl, 0.1M potassium acid phthalate, pH 4.0. Upper trace: $(HOCl)_o = 3.8 \times 10^{-5}$M. Lower trace: $(HOCl)_o = 1.5 \times 10^{-5}$M

made by the k_1 and k_2 pathways; correction for these contributions was made by subtraction of calculated rates for the competing reactions under the experimental conditions. The resulting rate law, determined over the concentration ranges $(H^+) = (0.1\text{-}2.0) \times 10^{-4}$ M, $(HOCl) = (0.5\text{-}4.0) \times 10^{-5}$ M, $(H_2O_2) = (1.0\text{-}4.0) \times 10^{-3}$ M, $(Cl^-) = (0.01\text{-}10) \times 10^{-3}$ M is:

$$dO_2/dt = k_2(HOCl)(H^+)(Cl^-)$$

with $k_2 = 3.5 \times 10^4$ $M^{-2}sec^{-1}$ at 25°, $\mu \simeq 10^{-3}$ M. Experimental data are given in Figures 8 and 9, and in Table III.

Efforts to eliminate the autoinhibition by reagent purification were unsuccessful; the effect is diminished by using meticulously cleaned glassware, suggesting inhibition is somehow dependent upon the surface of the reaction vessel. Autoinhibitory effects were not influenced by the addition of sodium salts of chlorite, chlorate, perchlorate, sulfate or phosphate ions, or by the presence of oxygen in the reaction solution. However, a strong cation dependence was evident, lithium ion causing strong inhibition and potassium ion causing slight inhibition relative to sodium ion. Silver and mercury salts did not appreciably alter the reaction rates. Further, the extent of these inhibitory effects was inversely dependent upon the concentrations of hydrogen peroxide and chloride ions, reaction by the k_2 pathway in solutions containing (H_2O_2) or $(Cl^-) > 4 \times 10^{-3}$ M showing negligible inhibition.

The effects of acetate and phthalate buffers on the reaction rate are complicated. Catalysis of the k_2 pathway occurs at high concentrations of hydrogen peroxide, but is apparently compensated for by concurrent inhibitory effects at lower peroxide concentration levels. Thus, for instance, at pH4 with $(H_2O_2) = 4.4 \times 10^{-3}$ M, $(Cl^-) = 2.4 \times 10^{-3}$ M, a ca. 5-fold increase in initial rate is measured in 0.025 M acetate buffer over the unbuffered reaction,

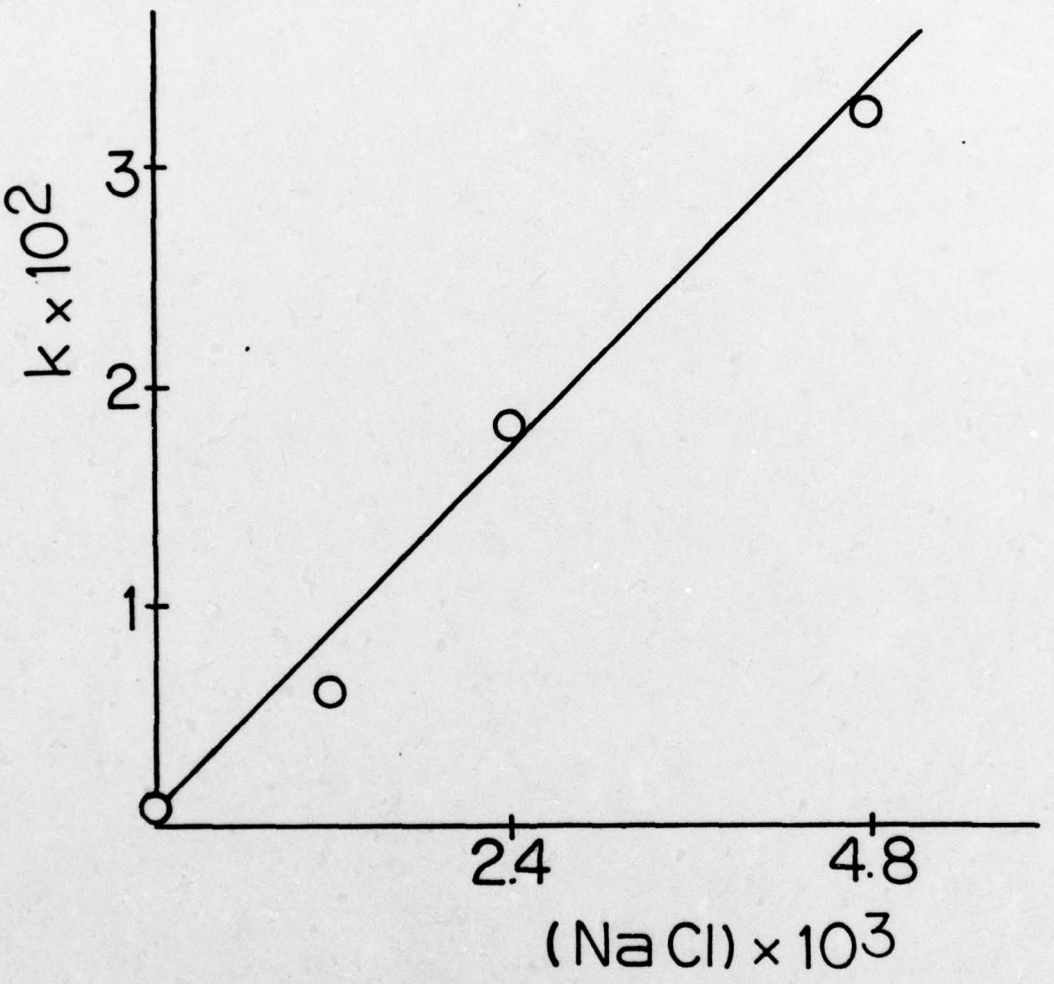

Figure 8. Chloride Ion Dependence of Reaction by Intermediate (k_2) Pathway. Rate constants, k, determined from initial oxygen evolution rate using $(dO_2/dt)_o = k(HOCl)_o$. Conditions: 0.0013M H_2O_2, pH 3.68

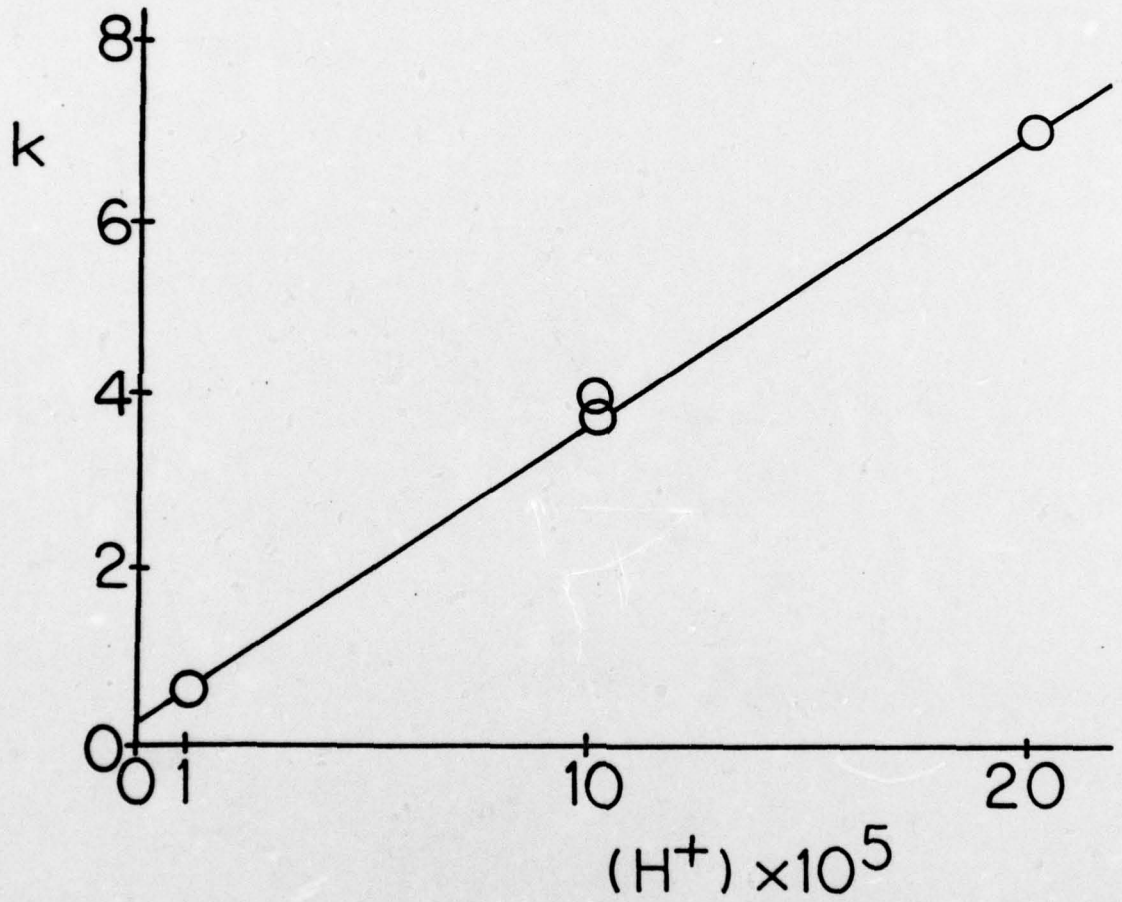

Figure 9. Hydrogen Ion Dependence of Reaction by the Intermediate (k_2) Pathway. Experimental points represent averages over 3 - 5 individual runs. Rate constants, k, calculated from initial oxygen evolution rates using $(dO_2/dt)_o = k(Cl^-)(HOCl)_o$.

Table III. Rate Constants (k_2) for the Intermediate Reaction

10^5(HOCl)	10^3(H_2O_2)	10^3(Cl^-)	10^5(H^+)	10^7·Initial Rate R_o(M sec^{-1})	$10^7 \cdot R_3$[a] (M sec^{-1})	$10^7 \cdot R_1$[b] (M sec^{-1})	$10^{-4} \cdot k_2$[c] ($M^{-2}sec^{-1}$)
2	1.32	4.86	20	6.44	0.144	0.113	3.2
"	"	"	"	6.40	"	"	"
"	"	2.43	"	3.7	0.139	0.059	3.6
"	"	1.21	"	1.16	0.135	0.030	1.91
"	"	"	"	1.08[d]	"	"	1.73
"	4.4	1.2	10	1.60	0.986	0.047	2.34
"	"	2.41	"	3.02	1.02	0.091	3.98
"	8.8	1.2	"	2.52	1.97	0.114	1.82
"	1.32	4.82	"	4.48	0.317	0.053	4.24
"	"	"	"	4.08	"	"	3.82
"	"	4.86	"	4.34	0.29	0.058	4.1
1	"	"	"	1.93	0.195	0.029	3.5
4	"	"	"	9.2	0.58	0.116	4.4
2	0.66	4.82	0.85	2.60[e]	2.1	0.0	6.1
"	"	"	"	2.38[f]	1.75	0.0	7.0
"	"	9.65	"	3.2[f]	1.75	0.0	8.8

[a] calculated from $R_3=k_3(H_2O_2)(OCl^-)$

[b] calculated from $R_1=k_1(H_2O_2)(Cl_2)$

[c] calculated from $k_2(HOCl)(H^+)(Cl^-)=R_o-R_3-R_1$

[d] direct measurement; all other rates determined by extrapolation of integrated rate data to t=0

[e] 0.1M phosphate buffer

[f] 0.025M phosphate buffer

whereas with $(H_2O_2) = 1.3 \times 10^{-3}$ M, $(Cl^-) = 4.8 \times 10^{-3}$ M only a ca. 20% increase is observed. With phthalate buffers the effects appear to be even more marked (Figure 7).

C. Determination of $^1\Delta$-Singlet Oxygen Yields by Chemical Trapping

1. General Procedures

Analysis of product yields in the presence of chemicals capable of selective reaction with electronically excited oxygen provides the means for determining the extent of its formation during oxidation of hydrogen peroxide. The approach can perhaps best be understood by considering the following minimal reaction scheme:

Scheme I:

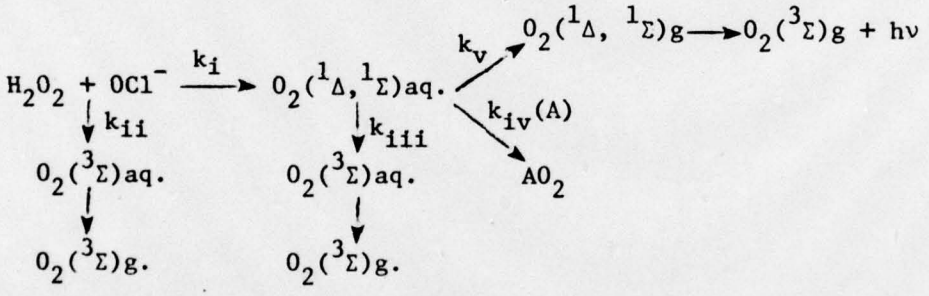

In this scheme, fractional yields of singlet oxygen initially formed (Y_1) are given by $Y_1 = k_i/(k_i+k_{ii})$. Yields of AO_2 formed during reaction (Y_{AO_2}) depend both upon Y_1 and upon partitioning of the intermediate over its various decomposition pathways, steps (iii)-(v), i.e.,

$$Y_{AO_2} = Y_1 \cdot \frac{k_{iv}(A)}{k_{iii}+k_{iv}(A)+k_v} \quad . \quad \text{In reciprocal form,}$$

$$Y_{AO_2}^{-1} = Y_1^{-1} \cdot [1+\beta/(A)] \text{ where } \beta = (k_{iii}+k_v)/k_{iv}.$$

The equations are formally analogous to those used in analysis of photosensitized generation of singlet oxygen (17): measurement of Y_{AO_2} as a function of (A) permits determination of Y_1, the information sought.

The compound 2,5-dimethylfuran (DMFu) was chosen as chemical trapping agent. Features which make the system attractive are the relatively high solubility of DMFu in aqueous media, its high selective reactivity towards $^1\Delta$-excited molecular oxygen, and its low reactivity towards H_2O_2 and HOCl, at least in alkaline solution.

2. The Alkaline (k_3) Pathway

Results for two reaction conditions are given in Figure 10. For all runs, DMFu concentrations were in sufficient excess to ensure that the factor $\beta/(A)$ remained constant over the course of the reaction. In general, both intercepts (Y_1^{-1}) and slopes ($Y_1^{-1} \cdot \beta$) of the double reciprocal plots are independent of medium conditions in the domain where the alkaline pathway predominates.

Quenching ratios ($\beta \simeq 5.5 \times 10^{-4}$) were slightly higher than the β-value determined by photosensitization methods ($\beta = 3 \times 10^{-4}$) for identical medium conditions. The latter number is identical to β-values cited in the literature (18) for methylene-blue sensitized singlet oxygen formation. The discrepancy in values in the two reactions may reflect differences in deactivation by escape into the gaseous phase (step v in Scheme I); molecular oxygen is evolved in the peroxide oxidation reaction, but is only consumed in the photochemical experiments. Alternatively, the presence of photosensitizer dye might alter relative rates of physical and chemical deactivation of "nascent" singlet oxygen.

Conditions for which hypochlorite consumption was extremely rapid (high H_2O_2 concentrations, pH 8-9.5) gave experimental quenching ratios (β) greater than those routinely encountered. The effect is likely ascribable to incomplete mixing of reactants giving rise to localized depletion of the trapping agent with attendant increases in measured O_2 yields. At considerably reduced hypochlorite reduction rates (low peroxide, low pH), the β-value undergoes an apparent decrease. This effect is artifactual, and has been shown to arise from the direct reaction of hypohalite with dimethylfuran. The competitive natures of hydrogen peroxide and DMFu reactions with hypohalite are illustrated

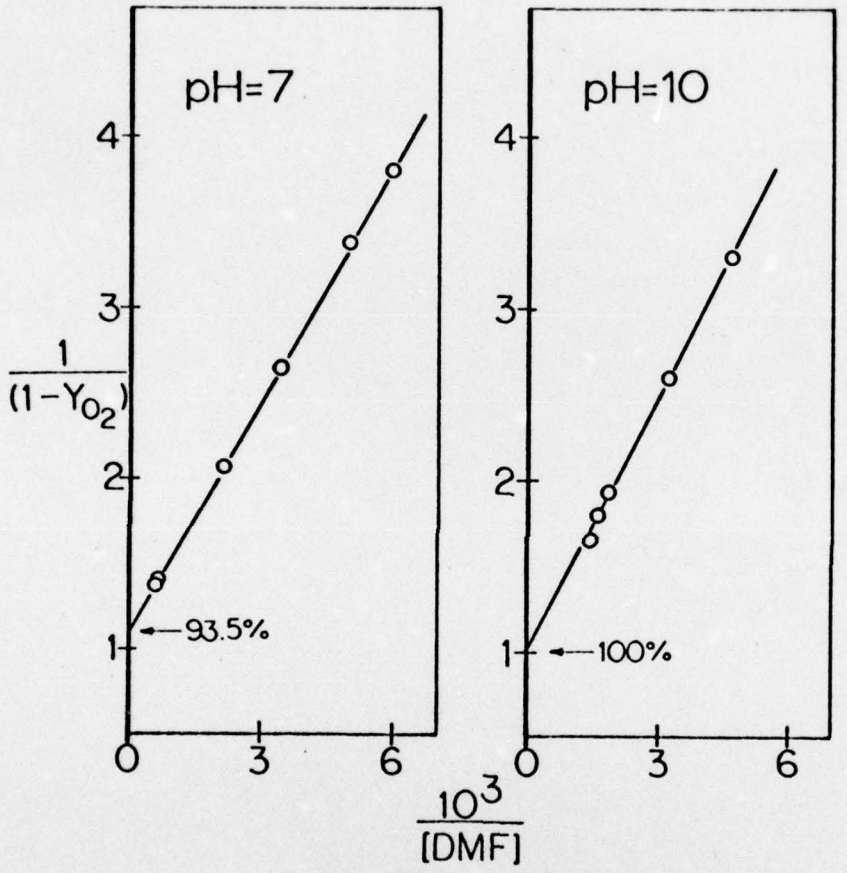

Figure 10. Competitive Quenching of Singlet Oxygen

in Figure 11, where it is shown that not only are oxygen yields reduced in the presence of DMFu, but the apparent rate constant for O_2 evolution also increases. Since the HOCl-DMFu reaction does not produce oxygen, this increase can only be attributed to competition between reductants for HOCl. Kinetic characterization of the HOCl-DMFu reaction is described below; decreases in oxygen yields in quenching experiments at low hypochlorite reduction rates can be quantitatively accounted for by this reaction.

It is pertinent to note that extrapolated singlet oxygen yields (Y_1) are insensitive to the apparent variations in β-values at the extreme reaction rates; results indicate essentially quantitative formation of singlet oxygen in the H_2O_2-HOCl reaction by the alkaline pathway.

Quenching experiments were also made for H_2O_2 oxidation by HOCl in aqueous-alcoholic mixtures and by Cl_2O in (nearly) anhydrous organic solvents; singlet oxygen yields (Y_1) are given in Table IV. Results cited for the organic media are only tentative since possible complications arising from the Cl_2O-DMFu reaction have not been considered and apparent acidities are unknown.

3. The Intermediate (k_2) Pathway

a. Oxidation of DMFu by HOCl

Interference in the quenching experiments by direct reaction of HOCl with the chemical trapping agent (Figure 11) becomes progressively greater with increasing acidities. Disappearance of DMFu exhibited complex kinetic behavior, highly dependent upon medium conditions and characterized by the formation and slow decay of unstable intermediate species (Figure 12). Nonetheless, under the conditions of the trapping experiments, the rate law could be cast in simple form, i.e.,

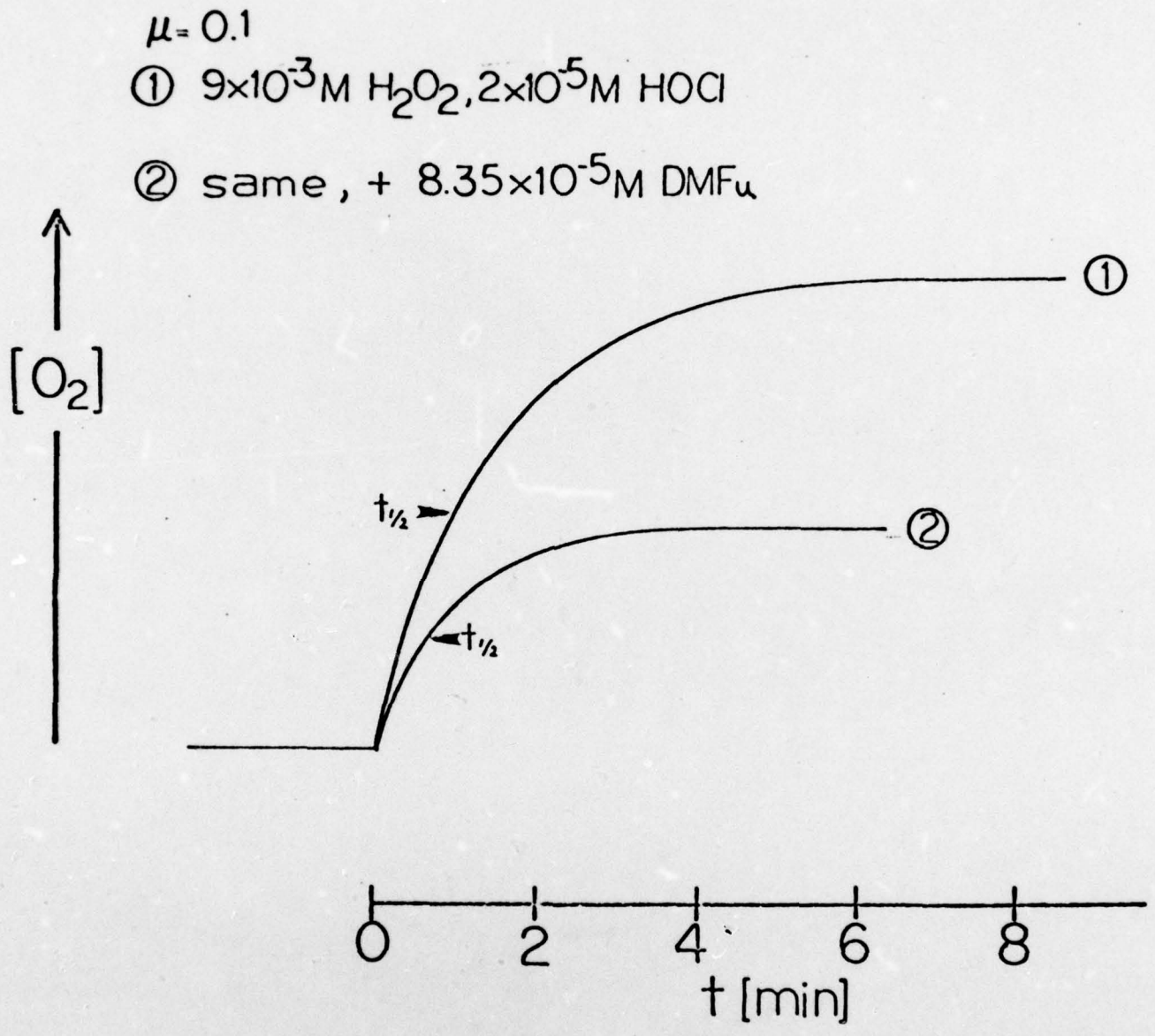

Figure 11. Oxygen Evolution Rate at pH 5.0 for the Alkaline (k_3) Pathway

Table IV. Singlet Oxygen Yields in Organic Solvents

Solvent	Y_1
Methanol:H_2O = 1:1, pH 8.25	0.86, 0.92
Ethanol:H_2O = 19:1	0.6 - 0.7
Methanol	0.6
Ethanol	0.7 - 0.8
Carbon Tetrachloride	0.2

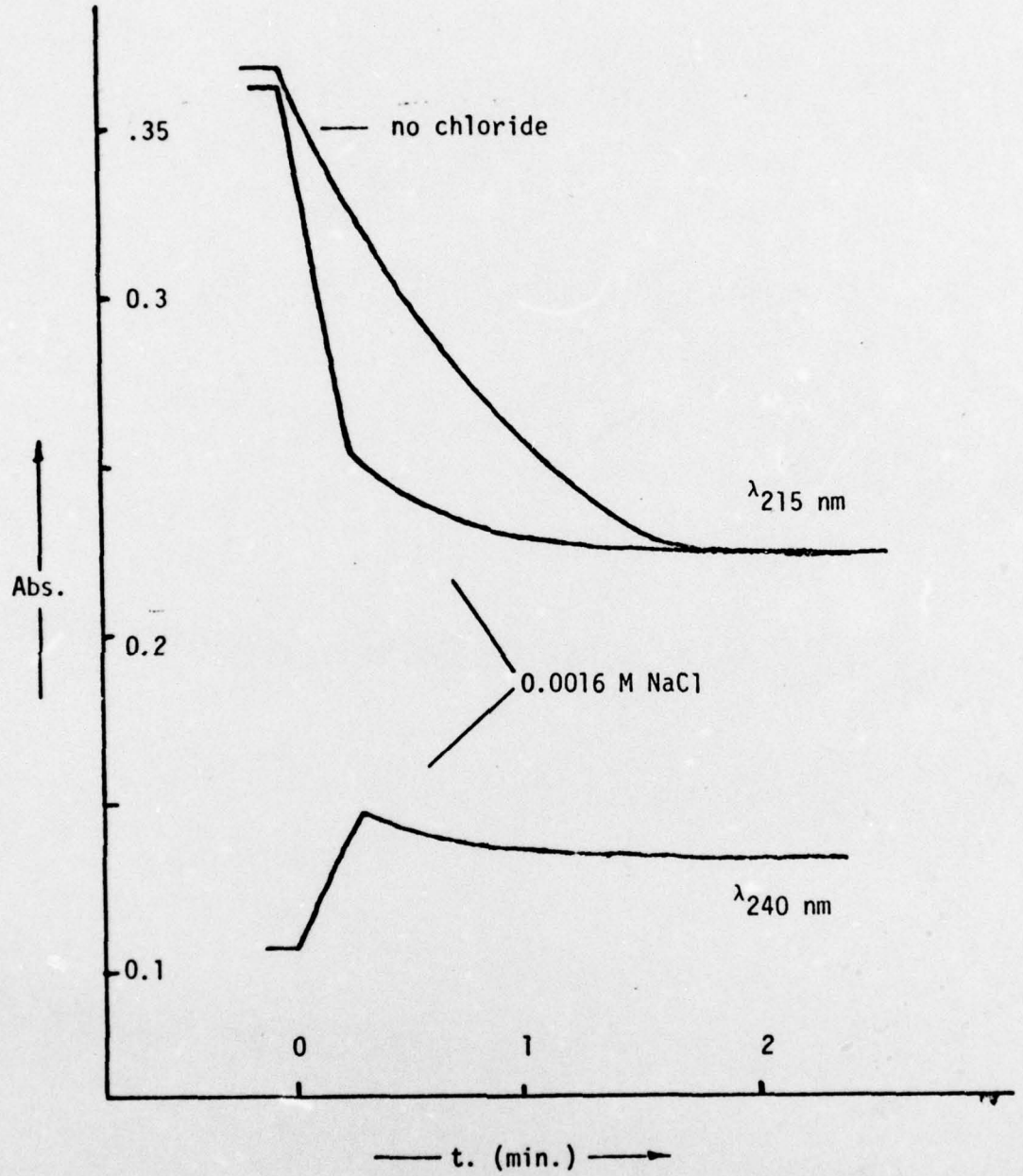

Figure 12. Oxidation of 2.5-Dimethylfuran by Hypochlorous Acid. Conditions: pH 4.0, 1cm optical cell, $(HOCl)_o = 2.5 \times 10^{-4}M$, $(DMFu)_o = 4.7 \times 10^{-5}M$. Upper trace: Absorbance at 215nm during reaction with HOCl. Lower trace: Absorbance at 240nm during reaction with HOCl + Cl^-. Absorbance changes show zero order loss of DMFu with concurrent formation of an unstable uv absorbing intermediate.

$$-d(DMFu)/dt = [k_c + k_d(Cl^-)](HOCl)(H^+)$$

with k_c = 93 $M^{-1}sec^{-1}$, $k_d = 4.2 \times 10^4 M^{-2}sec^{-1}$ at 25°, $\mu \simeq 10^{-3}M$. Note that the chlorine-dependent pathway, $k_d(HOCl)(H^+)(Cl^-)$, is identical to the rate law for the intermediate pathway for the $HOCl-H_2O_2$ reaction, i.e., $k_d = k_2$. This result strongly implies that the two reactions occur by rate-limiting formation of a common intermediate whose composition is H_2OCl_2.

b. Singlet Oxygen Trapping Experiments

Using procedures analogous to those described for the alkaline reaction we measured oxygen yields in solutions containing reactants and DMFu (Table V). Conditions were adjusted to optimize reaction by the intermediate (k_2) pathway. Thus, at pH 4.0, with $(Cl^-) = 7 \times 10^{-3}M$, $(H_2O_2) \simeq 0.018M$, 47% total reaction occurred through the intermediacy of $[H_2OCl_2]$.

In analyzing the data, the following concurrent reactions were considered:

(1) $H_2O_2 + Cl_2 \xrightarrow{k_1} O_2 + 2H^+ + 2Cl^-$

(2) $HOCl + H^+ + Cl^- \xrightarrow[\text{slow}]{k_2} [H_2OCl_2]$ $\xrightarrow{k_4(H_2O_2)} O_2 + H_2O + 2H^+ + 2Cl^-$; $\xrightarrow{k_5(DMFu)}$ oxidation products

(3) $H_2O_2 + OCl^- \xrightarrow{k_3} O_2 + H_2O + Cl^-$

(4) $HOCl + H^+ \xrightarrow[DMFu]{k_c}$ oxidation products

Under the experimental conditions, HOCl is concentration-limiting and reactions (1)-(4) exhibit simple exponential behavior. The fractions of the total reaction proceeding by any of the pathways can therefore be had from the ratios of the pseudo-first-order rate constants, e.g., for pathway (2) the ratio is $k_2'/\Sigma k_i$, where $\Sigma k_i = k_1' + k_2' + k_3' + k_c'$. Oxygen is formed by pathways (1)

and (3) and, partially, by pathway (2), depending upon the partitioning of the intermediate between steps (4) and (5). Finally, since reaction of $[H_2OCl_2]$ with H_2O_2 yields O_2, whereas reaction with DMFu does not, measurement of oxygen yields provides information on the relative reaction rates of the reductants with the intermediate. Since any singlet oxygen initially formed in the $[H_2OCl_2]$-H_2O_2 reaction will be partially trapped by reaction with DMFu, those experiments can also, in principle, measure the extent of singlet oxygen formation by the k_2 pathway.

Measured oxygen yields were corrected for oxygen formed by the acid and alkaline pathways using the equation:

$$\frac{O_2(\text{corr.})}{(HOCl)_o} = \frac{O_2(\text{meas.})}{(HOCl)_o} - \left(\frac{k_1' + k_3'}{\Sigma k_i}\right)\left[\frac{\beta/(A)}{1 + \beta/(A)}\right]$$

The ratio, $\beta/(A)/[1 + \beta/(A)]$, represents the fraction of singlet oxygen initially formed that is not chemically trapped by DMFu. It is tacitly assumed that reaction by the acid pathway gives rise to formation of singlet oxygen, although this is not known. Since reaction by this pathway comprises less than 10% of the total decomposition of HOCl, any errors introduced by the assumption are minor.

Results of the calculations given in Table V indicate that all the oxygen formed can be accounted for by the acid and alkaline reactions, hence that, by the k_2 pathway, DMFu competes effectively with H_2O_2 for the intermediate, $[H_2OCl_2]$, and therefore no information concerning singlet oxygen formation in the latter reaction can be had from these experiments.

4. The Acid (k_1) Pathway

Molecular chlorine reacts prohibitively rapidly with known water soluble trapping agents, precluding their use in singlet oxygen quenching experiments. No chemiluminescence was visible in this reaction domain even at optimal peroxide decomposition rates.

Table V. Oxygen Yields for the Intermediate Pathway*

Run #	O_2(meas.)/$(HOCl)_o$	$10^4 \cdot (A)(M)$	$(k_1' + k_3'/\Sigma k_i)[\beta/(A)/(1 + \beta/(A)]$	O_2(corr.)/$(HOCl)_o$
1	0.30	1.9	0.28	0.02
2	0.25	2.4	0.26	-0.01
3	0.25	2.8	0.24	0.01
4	0.22	2.8	0.24	-0.02
5	0.11	5.4	0.18	-0.07
6	0.10	5.7	0.18	-0.08
7	0.16	3.3	0.22	-0.06
8	0.14	3.0	0.24	-0.10

*At pH 4.0, $(Cl^-) = 7.0 \times 10^{-3}$M, $(H_2O_2) = 0.018$M, T=25°C. For these conditions, rates by pathways (1)-(4) are: $R_1 = k_1'(HOCl) = 0.0061(HOCl)$, $R_2 = 0.0294(HOCl)$, $R_3 = 0.0177(HOCl)$, $R_4 = 0.0093(HOCl)$; $(k_1' + k_3')/\Sigma k_i = 0.38$, $\beta = 5.0 \times 10^{-4}$.

V. Discussion

A. Mechanistic Considerations

1. Geometries of Activated Complexes

Thermodynamic parameters for reaction by the different pathways are given in Table VI. In each instance reactions are sufficiently exothermic to allow direct formation of molecular oxygen in its $^1\Delta$ electronic state. (Lowest excited states of O_2 are $^1\Delta$ and $^1\Sigma$, 22 and 38 kcal/mol, resp., above the ground electronic ($^3\Sigma$) state (19)). Because reactions by the various pathways are all highly exergonic, rates by the various pathways are not likely to be strongly influenced by their relative driving forces (20). In this regard, note that the relative rates do not vary systematically with reaction free energies (c.f., the reaction between OCl^- and HO_2^- which is undetectably slow, even in strongly alkaline solution where these ions are the dominant species (Figure 5).)

The kinetic data can be conveniently rationalized if it is assumed that reaction takes place by nucleophilic attack by peroxide upon the chlorine atom, forming, e.g., for the alkaline pathway, an activated complex whose geometry is $[HO_2\text{-}Cl\text{-}OH]^-$. Though unstable, this complex bears formal resemblance to the well-described trihalide ions. The central chlorine atom is electropositive; two electron transfer from peroxide leads directly to the reaction products, with both atoms of molecular oxygen being derived from the peroxide (21). Conservation of spin momentum requires that the oxygen product be singlet, as has now been demonstrated for the alkaline pathway.

The ion HO_2^- is strongly nucleophilic, as judged by its dynamic behavior towards electrophilic organic substrates (22), whereas H_2O_2 exhibits only weakly nucleophilic character. In HOCl, the chlorine atom is electropositive (23), polarization is weakened by removing a proton or substituting

Table VI. Thermodynamics of Hydrogen Peroxide Oxidation by Chlorine[a]

Reaction	$-\Delta G^\circ_{25^\circ}$ (kcal/mol)	$-\Delta H^\circ$ (kcal/mol)
$Cl_2 + H_2O_2 \longrightarrow O_2 + 2H^+ + 2Cl^-$	32.8	28.3
$HOCl + H_2O_2 \longrightarrow O_2 + H^+ + Cl^- + H\ O$	37.4	34.8
$OCl^- + H_2O \longrightarrow O_2 + Cl^- + H_2O$	47.6	38.0
$OCl^- + HO_2^- \longrightarrow O_2 + Cl^- + OH^-$	44.4	32.9
$HOCl + HO_2^- \longrightarrow O_2 + Cl^- + H_2O$	53.3	43.1

[a] Calculated from data given in ref. 27 and D. D. Perrin - "Dissociation Constants of Inorganic Acids and Bases in Aqueous Solution" - IUPAC publication, Butterworths, London (1969).

Cl^- for the OH^- ion. Therefore, the energetically least demanding means of reaching an activated complex for the redox reaction is by nucleophilic attack of HO_2^- upon HOCl at the electrophilic chlorine atom. For each of the other pathways the chlorine species (OCl^-, Cl_2) is a weaker electrophile and/or the attacking hydrogen peroxide is a poorer nucleophile. An additional factor mitigating against formation of the activated complex from OCl^- and HO_2^- is the electrostatic repulsion encountered by the like-charged ions. Two additional points are worth emphasizing:

(i) that the species we identify as reactive by the k_3 pathway (HO_2^-, HOCl) are not the ones that predominate in solution (H_2O_2,OCl^-) and, therefore, that the reaction as formulated in pathway b (Sect. IV. B.1) is correct, and

(ii) that our postulations are consistent with previously proposed mechanisms for the acid pathway(s) in which a HOOCl intermediate is thought to form by nucleophilic displacement of Cl^- by H_2O_2.

2. Is Singlet Oxygen Formed in Oxidation of H_2O_2 by Molecular Chlorine?

A free-radical mechanism for peroxide decomposition by the acid pathway has been proposed (24), the essential features of which are sequential one-electron transfers from peroxide to chlorine species as in the following equations:

$$H_2O_2 + Cl_2 \underset{k_{-1}}{\overset{k_1}{\rightleftharpoons}} H_2O_2^+ + Cl_2^- \xrightarrow{k} O_2 + 2H^+ + 2Cl^-$$

In order to derive the experimental rate law, it was necessary to assume that chain-propogating steps, e.g.,

$$Cl_2^- + H_2O_2 \longrightarrow 2Cl^- + H_2O_2^+$$

$$H_2O_2^+ + Cl_2 \longrightarrow O_2 + 2H^+ + Cl_2^-$$

are insignificant. From published kinetic data (25), the value for the radical-initiating step was calculated to be $k_1 = 1.9 \times 10^2 M^{-1} sec^{-1}$. This mechanism

provides an attractive explanation for the apparent absence of chemiluminescence in reaction by the acid pathway since stepwise electron transfer allows the direct formation of $^3\Sigma$ molecular oxygen without violation of spin conservation requirements. On the other hand, there is no reason to suspect formation of $^1\Delta$ oxygen is energetically restrictive (Table VI).

In any event, the mechanism can be shown to be incorrect. The equilibrium constant for the first electron transfer step,

$$K = k_1/k_{-1} = (H_2O_2^+)(Cl_2^-)/(H_2O_2)(Cl_2),$$

can be calculated from the following thermodynamic data:

(5) $\frac{1}{2}\ Cl_2 \rightleftharpoons Cl\cdot_{aq.}$, $K_5 = 1.7\times10^{21} M^{\frac{1}{2}}$ (ref. 25,26)

(6) $H_2O_2 + \frac{1}{2}\ Cl_2 \rightleftharpoons HO_2\cdot + H^+ + Cl^-$, $K_6 = 4.3\times10^{-3} M^{3/2}$ (ref. 27)

(7) $Cl\cdot + Cl^- \rightleftharpoons Cl_2^-$, $K_7 = 1.9\times10^{5} M^{-1}$ (ref. 28)

(8) $H_2O_2^+ \rightleftharpoons HO_2\cdot + H^+$, $K_8 \simeq 10^{-1} M$ (ref. 29)

for which $K = K_5\cdot K_6\cdot K_7/K_8 \simeq 1.4\times10^{-17}$. To account for these thermodynamic properties, the rate constant $k_{-1} = k_1/K \simeq 10^{19} M^{-1}sec^{-1}$, far too fast to be physically attainable.

It is clear, then, that any free radical mechanism must include chain-propagating steps. In testing numerous reaction schemes, we have not found such a mechanism capable of reproducing the experimental rate law. There are presently no plausible arguments favoring the intermediacy of radical species in this reaction.

Assuming that singlet-excited oxygen is formed in the H_2O_2-Cl_2 reaction, how can we explain the absence of detectable chemiluminescence? Maximal steady-state concentrations of $^1\Delta$-oxygen can be estimated from a single kinetic model comprising exponential growth and decay of the intermediate, i.e., for the acid pathway, $O_2(^1\Delta) = [k_1'(HOCl)_o/(k_\tau - k_1')][\exp(-k_1 t_{max}) - \exp(-k_\tau t_{max})]$,

where t_{max} is the time after mixing corresponding to the maximal concentration of $O_2(^1\Delta)$, $k_1' = k_1(H_2O_2)_o$ and $k_\tau = 1/\tau$, with τ = 2 μsec being the lifetime of $O_2(^1\Delta)$ in aqueous solution (30). An equivalent expression holds for the alkaline (k_3) pathway. Values of t_{max} are obtained by evaluating the first derivative of the equation at $d(^1\Delta)/dt = 0$. For the conditions of the chemiluminescence experiments, the ratio of maximal singlet oxygen concentrations by the two pathways is $(^1\Delta)_{k_1}/(^1\Delta)_{k_3} \simeq 0.06$. Since visible chemiluminescence occurs principally by dimol emission (31), intensities are proportional to the square of $^1\Delta$-concentrations (32). Relative intensities for the two pathways are calculated to be: $I_{k_1}/I_{k_3} \simeq 0.004$. An alternative model based upon the observation that dimol emission occurs from the gas phase (33) and, therefore, that $^1\Delta$-O_2 concentrations should be roughly proportional to oxygen evolution rates gives equivalent results. Neither calculation should be taken literally since, at the high concentrations of reactants used, the rapid reaction rates encountered obviate any attempts at achieving homogeneous mixing. It is evident, even from this crude analysis, however, that chemiluminescence intensities for the H_2O_2-Cl_2 reaction cannot exceed ca. 1% of the intensities attainable by the H_2O_2-HOCl pathway.

3. The Intermediate (k_2) Pathway - Evidence for a "Chlorenoid" Mechanism

The rate law for the DMFu-HOCl reaction is consistent with rate data for HOCl oxidation of other similarly reactive organic molecules (34). In particular, the term $k_2(HOCl)(H^+)(Cl^-)$ is commonly found, implying rate-limiting formation of an activated chlorine intermediate which is identical to the one involved in oxidation of H_2O_2 by the k_2 pathway. We believe that chlorine hydrolysis (equation 9) also proceeds by rate limiting formation of this same intermediate.

Eigen and Kustin (35) have interpreted their kinetic data for this

reaction in terms of the following scheme:

$$(9a)\quad Cl_2 + H_2O \underset{k_{31}}{\overset{k_{13}}{\rightleftharpoons}} HOCl_2^- + H^+ \underset{k_{43}}{\overset{k_{34}}{\rightleftharpoons}} HOCl + H^+ + Cl^-$$

(rate constants refer to their notation). Alternative pathways were excluded on the basis of kinetic and thermodynamic arguments. The intermediate, $HOCl_2^-$, was not observed, but its existence is consistent with other kinetic data (36) and is structurally analogous to other, stable halogen species, e.g., the trihalide ions.

We differ with Eigen and Kustin on the following point. They assert that proton transfer to $HOCl_2^-$, i.e.,

$$(10)\quad H_3O^+ + HOCl_2^- \underset{k_r}{\overset{k_f}{\rightleftharpoons}} H_2O + H_2OCl_2$$

is energetically favorable, hence, rapid (37); we feel that reaction (10) is energetically unfavorable in the direction written and, therefore, that proton transfer to $HOCl_2^-$ is necessarily slow. The mechanistic consequence of this interpretation is the recognition of H_2OCl_2 as the least-stable intermediate, viz., the reaction scheme:

$$(9b)\quad Cl_2 + H_2O \underset{k_{31}}{\overset{k_{13}}{\rightleftharpoons}} H_2OCl_2 \underset{k_{43}}{\overset{k_{34}}{\rightleftharpoons}} HOCl + H^+ + Cl^-$$

Their kinetic analysis remains valid, but now the elementary step identified by k_{43} refers to H_2OCl_2 formation; by their analysis, $k_{43} \simeq 2\times10^4 M^{-2} sec^{-1}$, identical to k_2 within the limits of the estimation.

Some estimate of the relative strengths of the bases in equation (10) can be had from consideration of thermodynamic calculations for the equilibrium:

$$(11)\quad X_{2_{aq}} + H_2O \rightleftharpoons H_2OX^+_{aq} + X^-_{aq}$$

for which $K_{11} \simeq 10^{-30}$ M (38). When combined with the equilibrium constant for chlorine hydrolysis (eq. 9, $K_9 = 4\times10^{-4} M^2$), the data allows calculation of the acid dissociation constant, $K_a = (HOCl)(H^+)/(H_2OCl^+) = K_{10}/K_{11} \simeq 4\times10^{26}$ M. Comparison with the analogous constant for dissociation of the hydronium ion, $K'_a = (H_2O)(H^+)/(H_3O^+) = 55$ M, reveals the enormous base-weakening effect of chlorine

substitution for hydrogen on oxygen. Although addition of a chloride ion in forming $HOCl_2^-$ will increase basicity at the oxygen atom, it seems unlikely that total compensation can be achieved. We therefore anticipate that, in equation (10), $k_r \approx 10^{10} sec^{-1}$ with k_f determined by the difference in base strengths of H_2O and $HOCl_2^-$ (38).

A unified view of these reactions, consistent with available kinetic data, is given in Scheme II.

Scheme II.

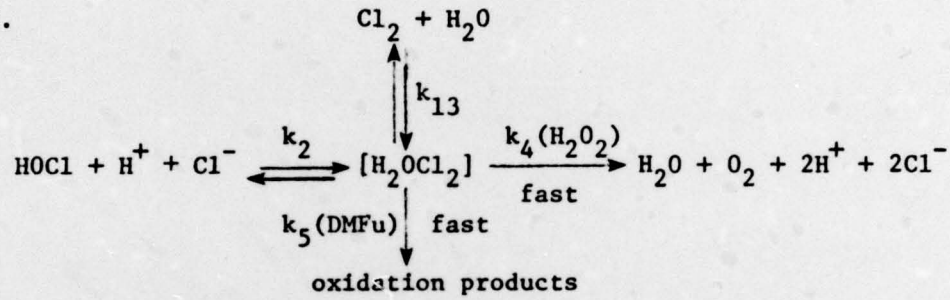

Considering the chlorine hydrolysis reaction, a likely geometry for the intermediate is H_2O-Cl-Cl. The Cl-O bond is considerably weakened by the two bound protons, leading to facile dissociation of H_2O. The central chlorine atom is also electron-deficient and is activated both towards reduction and electrophilic insertion into electron-rich bonds. In this latter regard, the behavior of the intermediate can be thought to parallel that proposed for insertion reactions involving electrophilic oxygen (oxenoid mechanism (39)) and carbon atoms (carbenoid mechanism (40)).

The inhibitory and catalytic effects observed in the H_2O_2- HOCl reaction by the k_2 pathway are reminiscent of similar reports by Connick (5) and Kajiwana and Kearns (3), in the latter instance for the alkaline reaction in D_2O. Although considerably more work will be required to identify sources of these effects, several points are worth mentioning. First, the reaction stoichiometry remains unaltered, even under conditions of strong inhibition of rates.

It is clear that intermediates ultimately react to give O_2 product. Second, apparent surface effects may relate to borate inhibition of the alkaline pathway, especially since the effects are diminished at high concentration levels of H_2O_2. Third, the rate-enhancing effects of acetate and phthalate buffers may well arise by general acid catalysis, which would be expected for rate-limiting proton transfer as we have proposed for formation of the reactive H_2OCl_2 intermediate.

B. Implications for Gas-Phase Singlet Oxygen Generation

Chemiluminescence arising from $^1\Delta$-O_2 dimol emission is most intense for reaction in alkaline aqueous solutions (3). We have shown that under these conditions singlet oxygen is the exclusive oxygen product of the primary redox reaction. *Optimization of gaseous singlet oxygen yields therefore depends only* upon finding the means for minimizing its deactivation by solvent.

By combining rapid mixing and cryogenic pumping of concentrated HOCl and H_2O_2 we have been able to transfer detectable amounts of singlet oxygen into the gas phase. Considerable improvement in the engineering design of the reactor (Figure 2) would probably allow for substantial increases in transfer efficiencies. Addition of organic solvents to ca. 50% might improve yields by decreasing rates of physical quenching (30) while not materially affecting rates of singlet oxygen formation. Although singlet oxygen lifetimes in nonaqueous solvent mixtures are much greater than in water, the use of these solvents is not feasible because they are often reactive towards H_2O_2 and Cl_2O and, more importantly, oxidation-reduction rates and possibly primary singlet oxygen yields (Table IV) are markedly reduced. Finally, the addition of very high concentrations of ionic salts might provide for improved yields by decreasing the "effective" solvent concentrations and volatility, and by decreasing oxygen solubilities.

Ultimately, it is clear that the prospects for obtaining high yields (>50%) of gaseous singlet oxygen rest upon improving means of degassing products formed and/or development of solid-phase reactions or reactions capable of going rapidly to completion at low temperatures.

VI. Suggestions for Future Studies

A. Mechanisms of Solution Quenching of $^1\Delta$-Oxygen

Having determined rates for singlet oxygen formation, it becomes possible to obtain information regarding the relative rates of oxygen quenching and escape to the gas phase, steps (iii) and (v) in Scheme I. The basic experiment consists of measuring chemiluminescence arising from dimol emission of $^1\Delta$-oxygen under varying reaction conditions, it being generally understood that luminescence intensities are proportional to singlet oxygen concentrations in the gas phase (33). Two types of studies would be particularly useful:

(1) Reaction over varying medium conditions for which rates of singlet oxygen formation are maintained constant. Variations in chemiluminescence intensities will give indication of the effect of altering solvent structure upon relative rates of quenching and gas formation.

(2) Reaction in a constant medium in which rates of singlet oxygen formation are varied. Since solution deactivation of $^1\Delta$-oxygen occurs by simple exponential decay[17], the experiments will permit evaluation of the "apparent" reaction order for gas-phase escape.

Additional experiments which probe the effect of reaction medium upon singlet oxygen dynamics over a wider range should be undertaken, both involving varying chemical composition of the ionic medium and use of non-aqueous solvents. It may be required in each of the systems to determine primary singlet oxygen yields before chemiluminescence behavior can be interpreted, but it is anticipated that these studies could be rapidly accomplished now that the basic methodology has been established.

B. Reactions Using Other Oxidants

The alternative use of HOBr as oxidant should be explored, particularly in mixed solvents containing high percentages of organic solvents.

Because H_2O is an especially efficient quencher of singlet-excited oxygen, attempts should be made to minimize the quantity of water in reactant hypochlorite solutions. Use of anhydrides of hypochlorous acid would be advantageous, providing a high reaction rate can be maintained. The reaction rate of anhydrides with peroxides presumably depends upon the rate of hydrolysis of the anhydride into hypochlorite and acid (or salt). A wide range of anhydrides of varying, but mostly very low stability, might prove suitable. Some examples are CH_3CO_2Cl, HCO_2Cl, CO_3SOCl, O_2NOCl, and Cl_2O.

Novel methods of singlet oxygen production based on the thermal decomposition of highly unstable oxygenated compounds, such as endoperoxides (41) may become feasible in the near future as our understanding of the properties of such compounds grows.

VII. References

1. R. J. Browne and E. A. Ogryzlo, Can. J. Chem., 43, 2915 (1965).
2. A. U. Khan and M. Kasha, J. Am. Chem. Soc., 92, 3293 (1970).
3. T. Kajiwara and D. R. Kearns, J. Am. Chem. Soc., 95, 5886 (1973).
4. Original proposal, Section III.A, pp. 3-4.
5. R. E. Connick, J. Am. Chem. Soc., 69, 1509 (1947).
6. G. Dulz and N. Sutin, Inorg. Chem., 2, 917 (1963).
7. E. A. Ogryzlo and A. E. Pearson, J. Phys. Chem., 72, 2913 (1968).
8. W. J. Wingo and G. M. Emerson, Anal. Chem., 47, 351 (1975).
9. I. M. Kohltoff and R. Belcher, Volumetric Analysis, Vol. III, Wiley Interscience, (New York) (L957, pp. 262 ff).
10. G. H. Cady, Inorg. Syntheses, 5, 156 (1957).
11. K. Bergmann and C. T. O'Konski, J. Phys. Chem. 67, 2169 (1963).
12. B. Makower, Thesis, University of California (Berkeley), 1932.
13. J. C. Morris, J. Phys. Chem., 70, 3798 (1966).
14. M. G. Evans and N. Uri, Trans. Faraday Soc., 45, 224 (1949).
15. D. M. Kern, J. Amer. Chem. Soc., 77, 5488 (1955).
16. L. Erdey and J. Inczedy, Acta Chim. Sci. Hung., 11, 125 (1957).
17. C. S. Foote, Accounts Chem. Research 1, 104 (1968). and references therein.
18. Y. Usui and K. Kamogawa, Photochem. Photobiol. 19, 245 (1975).
19. cf. D. R. Kearns, Chem. Reviews, 71, 395 (1971).
20. G. P. Hammond, J. Amer. Chem. Soc. 77, 334 (1955).
21. A. E. Cahill and H. Taube, J. Amer. Chem. Soc., 74, 2312 (1952).
22. cf. W. P. Jencks, "Catalysis in Chemistry and Enzymology," McGraw Hill, New York (1969), p. 193 ff.
23. J. Jander, Z. anorg. allgem. Chem., 280, 276 (1955).
24. G. Davies and K. Kustin, Inorg. Chem., 12, 961 (1973).

25. W. H. Woodruff and D. W. Margerum, Inorg. Chem., 12, 961 (1973).

26. Nat. Bur. Stand. (U.S.) Tech. Note, No. 270-3 (1968).

27. W. M. Latimer, "Oxidation Potentials," 2nd Ed., Prentice-Hall, Englewood Cliffs, New Jersey (1952).

28. G. G. Jayson, B. J. Parsons and A. J. Swallow, J. Chem. Soc. Faraday Trans. II, 69, 1597 (1973).

29. B. H. J. Bielski and J. M. Gebicki, Advan. Radiat. Chem., 2, 177 (1970).

30. P. B. Merkel and D. R. Kearns, J. Amer. Chem. Soc., 94, 7244 (1972).

31. S. J. Arnold, E. A. Ogryzlo and H. Witzke, J. Chem. Phys., 40, 1769 (1964).

32. R. J. Browne and E. A. Ogryzlo, Can. J. Chem., 43, 2915 (1965).

33. A. U. Khan and M. Kasha, J. Amer. Chem. Soc., 92, 3293 (1970).

34. cf. E. Berliner, J. Chem. Ed., 43, 124 (1966).

35. M. Eigen and K. Kustin, J. Amer. Chem. Soc., 84, 1355 (1962).

36. M. Anbar and H. Taube, J. Amer. Chem. Soc., 80, 1073 (1958).

37. M. Eigen, Angew. Chem., Internat. Ed., 3, 1 (1964).

38. R. P. Bell and E. Gelles, J. Chem. Soc., 2734 (1951).

39. cf., G. A. Hamilton in "Progress in Bioorganic Chemistry", Vol. 1, (E. T. Kaiser and F. J. Kezdy, Eds.) Wiley, New York (1971), p. 83.

40. cf., J. March, "Advanced Organic Chemistry," McGraw-Hill, New York (1968), p. 643 ff.

41. cf. H. R. Wasserman and J. R. Scheffer, J. Amer. Chem. Soc., 89, 3073 (1967).